Dynamics and bifurcations of a three-dimensional piecewise-linear integrable map

2004 J. Phys. A: Math. Gen. 37 12041

(http://iopscience.iop.org/0305-4470/37/50/007)

INSTITUTE OF PHYSICS PUBLISHING JOURNAL OF PHYSICS A: MATHEMATICAL AND GENERAL

J. Phys. A: Math. Gen. **37** (2004) 12041–12058 PII: S0305-4470(04)86294-2

Dynamics and bifurcations of a three-dimensional piecewise-linear integrable map

J M Tuwankotta[1,2], G R W Quispel[1] and K M Tamizhmani[3]

[1] A.R.C. Centre of Excellence for Mathematics and Statistics of Complex Systems, Mathematics Department, La Trobe University, Victoria 3086, Australia
[2] Department of Mathematics, Bandung Institute of Technology, Jl. Ganesa no. 10, Bandung, Indonesia
[3] Department of Mathematics, Pondicherry University, Kalapet, Pondicherry, 605 014, India

E-mail: R.Quispel@latrobe.edu.au, theo@dns.math.itb.ac.id and tamizh@yahoo.com

Received 15 September 2004, in final form 11 October 2004
Published 1 December 2004
Online at stacks.iop.org/JPhysA/37/12041
doi:10.1088/0305-4470/37/50/007

Abstract

In this paper, we consider a four-parameter family of piecewise-linear ordinary difference equations (OΔEs) in $\mathbb{R}^3$. This system is obtained as a limit of another family of three-dimensional integrable systems of OΔEs. We prove that the limiting procedure sends integrals of the original system to integrals of the limiting system. We derive some results for the solutions such as boundedness of solutions and the existence of periodic solutions. We describe all topologically different shapes of the integral manifolds and present all possible scenarios of transitions as we vary the natural parameters in the system, i.e. the values of the integrals.

PACS numbers: 02.30.Ik, 02.30.Oz, 05.45.−a, 47.20.Ky

1. Introduction

Integrable dynamical systems have been the subject of investigation for considerable time. The motion (or dynamics) in such systems is regular and 'well behaved' in contrast to chaotic systems. Despite the fact that most dynamical systems found in applications are non-integrable, insight from integrable systems is still very important. It provides us with a good starting point for dealing with non-integrable systems by looking at them, for example, as perturbations of integrable systems.

1.1. Piecewise-linear discrete systems and cellular automata

In [8], Tokihiro *et al* introduced a special transformation involving a limiting procedure with the aim of describing a direct connection between cellular automata and integrable nonlinear wave

equations. For their purpose, the parameters and the variables were assumed to be integers. A generalization of this concept by looking at real-valued parameters and real-valued variables is done e.g. in [4, 7]. This generalization leads to systems which are dynamically interesting in their own right. It provides us with the possibility of studying the topological changes of solutions since we can consider smooth changes in parameter space. However, the results for the cellular automata case can be constructed from our results here.

1.2. Summary of the results

In this paper we consider a dynamical system in $\mathbb{R}^3$ of the form

$$\overline{u} = v, \qquad \overline{v} = w, \qquad \overline{w} = uf(v, w), \tag{1.1}$$

which is integrable in the following sense. The system possesses two functionally independent integrals (real-valued functions in the state variables which are conserved under the mapping) and an invariant measure. Inspired by the study in [4, 7], we apply the same transformation involving a limiting procedure as in [8]. The first question we ask is whether the limiting system is also integrable. In the appendices of this paper we prove that the transformation and the limiting procedure send integrals of the original system to integrals of the limiting system.

As a case study, we consider a special rational function for f, namely

$$f(v, w) = \frac{\alpha + \beta v + \gamma w + \delta vw}{\alpha + \beta w + \gamma v + \delta vw}, \tag{1.2}$$

where α, β, γ and δ are real numbers. For $\alpha = 0 = \delta$, this map reduces to the three-dimensional MKdV mapping (see appendix A of [3]). For $\delta = 0 = \gamma$, the map reduces to a map that can be obtained from equation (37) of [5]. We have constructed the generalization (1.2), in order to have more parameters at our disposal. After applying the transformation and the limiting procedure, we have a piecewise-linear, volume-preserving, three-dimensional dynamical system possessing two piecewise-linear integrals.

We prove that the intersection between the two integral manifolds is almost everywhere transversal. This leads to the conclusion that the two integrals are functionally independent. Thus, the transformation and the limiting procedure do not destroy the integrability. Moreover, all solutions are bounded. Together with a special symmetry of the system, the boundedness of solutions implies the existence of periodic solutions in the system. Furthermore, realizing that the solution lives in a polygon-shaped intersection between the integral manifolds, we prove that all solutions in a polygon containing a periodic solution are periodic with the same period. As a consequence, we conclude that each integral manifold is fibred by polygons in which either periodic or quasi-periodic motions take place. This suggests that a good way for analysing the system in generality would be by fixing one of the integral manifolds and restricting the dynamics to that manifold. The solutions then live on the invariant polygons which are parametrized by the value of the other integral (which is still free).

For comparison, think of a planar nonlinear Hamiltonian flow which preserves all circles (centred at the origin). The phase space ($\mathbb{R}^2$) is fibred by these circles on which either periodic or quasi-periodic motions take place. The nontrivial invariant circles are diffeomorphic to each other, while in our case, some of the invariant polygons are topologically different. Although there is not much change in the dynamics, we consider this as a bifurcation of solutions.

There are two sources for these topological changes. The first is the non-smoothness of the integral manifold. We present four types of topological changes that occur in our case study in this paper. The second source is the fact that as we vary the value of the integral, the topological shape of the integral manifold might change. For this, we have listed all possible

scenarios for the shape of one of the integrals. Similar results can be derived for the second integral.

2. Problem formulation

Consider $\mathbb{R}^3$ with coordinates (u, v, w). We consider a four-parameter family of discrete dynamical systems which is defined by the mapping

$$\overline{u} = v, \qquad \overline{v} = w, \qquad \overline{w} = u\frac{\alpha + \beta v + \gamma w + \delta vw}{\alpha + \beta w + \gamma v + \delta vw} \equiv F(u, v, w), \tag{2.1}$$

where α, β, γ and δ are real numbers. This mapping has several properties.

(P_1) For all parameter values, the mapping (2.1) possesses two integrals (functions which are invariant under the mapping), i.e.

$$H_1 = \alpha(u + v + w) + \beta(uv + vw) + \gamma uw + \delta uvw, \tag{2.2}$$

and

$$H_2 = \delta\left(\frac{1}{u} + \frac{1}{v} + \frac{1}{w}\right) + \beta\left(\frac{1}{vw} + \frac{1}{uv}\right) + \frac{\gamma}{uw} + \frac{\alpha}{uvw}. \tag{2.3}$$

These integrals are *functionally independent*, i.e. the tangent planes of H_1 and H_2 are transversal almost everywhere.

(P_2) The mapping (2.1) is measure preserving (with a measure density function $m(u, v, w) = (uvw)^{-1}$), since

$$\det\begin{pmatrix} 0 & 1 & 0 \\ 0 & 0 & 1 \\ \frac{\partial F}{\partial u} & \frac{\partial F}{\partial v} & \frac{\partial F}{\partial w} \end{pmatrix} = \frac{\alpha + \beta v + \gamma w + \delta vw}{\alpha + \beta w + \gamma v + \delta vw} = \frac{\overline{w}\,\overline{v}\,\overline{u}}{wvu},$$

which then, together with the two (functionally independent) integrals, implies that the mapping (2.1) is integrable.

(P_3) The system is invariant under the transformation $(u, v, w) \leftrightarrow (\overline{w}, \overline{v}, \overline{u})$. This symmetry is also known as time-reversal symmetry.

(P_4) The system is invariant under the transformation in phase space: $(u, v, w) \mapsto (1/u, 1/v, 1/w)$ together with the transformation in parameter space $(\alpha, \beta, \gamma, \delta) \mapsto (\delta, \beta, \gamma, \alpha)$.

(P_5) The system is invariant under the transformation in phase space: $(u, v, w) \mapsto (\lambda u, \lambda v, \lambda w)$ together with the transformation in parameter space $(\alpha, \beta, \gamma, \delta) \mapsto (\mu\lambda^3\alpha, \mu\lambda^2\beta, \mu\lambda^2\gamma, \mu\lambda\delta)$.

2.1. Derivation of the piecewise-linear mapping

Let us now consider the transformations in the phase space

$$u \mapsto \exp\left(\frac{x}{\varepsilon}\right), \qquad v \mapsto \exp\left(\frac{y}{\varepsilon}\right), \qquad w \mapsto \exp\left(\frac{z}{\varepsilon}\right), \tag{2.4}$$

and also in the parameter space

$$\alpha \mapsto \exp\left(\frac{a}{\varepsilon}\right), \qquad \beta \mapsto \exp\left(\frac{b}{\varepsilon}\right), \qquad \gamma \mapsto \exp\left(\frac{c}{\varepsilon}\right), \qquad \text{and} \quad \delta \mapsto \exp\left(\frac{d}{\varepsilon}\right). \tag{2.5}$$

By using the identity

$$\lim_{\varepsilon\to 0} \varepsilon \ln\left(\exp\left(\frac{A}{\varepsilon}\right) + \exp\left(\frac{B}{\varepsilon}\right)\right) = \max(A, B),$$

we obtain the limit of the transformed equation in (2.1):

$$\overline{x} = y, \qquad \overline{y} = z, \qquad \overline{z} = x + g(y, z) \tag{2.6}$$

where $g(y, z) = \max(a, b+y, c+z, d+y+z) - \max(a, b+z, c+y, d+y+z)$. Similarly, in the limit, the transformed integrals (2.2) and (2.3) become

$$I_1 = \max(a+x, a+y, a+z, b+x+y, b+y+z, c+x+z, d+x+y+z), \tag{2.7}$$

and

$$I_2 = \max(d-x, d-y, d-z, b-y-z, b-x-y, c-x-z, a-x-y-z). \tag{2.8}$$

The following are properties of the system (2.6). It is instructive to compare these with the properties of the original system (2.1).

- (P'_1) It can easily be checked that (2.7) and (2.8) are integrals of (2.6). In appendix A we prove this for slightly more general systems (see theorem A.1). Although both H_1 and H_2 are transformed into integrals of the transformed system (A.3) by theorem A.1, in general they need not be functionally independent. In the following section we will show that for our case, the two integrals mentioned above are functionally independent.
- (P'_2) The system (2.6) is volume preserving. This can be proved by computing the determinant of the Jacobian matrix of (2.6) but one needs to be careful to exclude the points where the derivative is not defined. Moreover, the Jacobian of the mapping (2.6) at the point, where it is well defined, is positive. This implies that *the mapping (2.6) is orientation preserving*.
- (P'_3) The system (2.6) also has time-reversal symmetry.
- (P'_4) The system (2.6) is invariant under the transformation in phase space: $(x, y, z) \mapsto (-x, -y, -z)$ together with the transformation in parameter space $(a, b, c, d) \mapsto (d, b, c, a)$.
- (P'_5) The system is invariant under the transformation in phase space: $(x, y, z) \mapsto (x+\lambda, y+\lambda, z+\lambda)$ together with the transformation in parameter space $(a, b, c, d) \mapsto (a+3\lambda+\mu, b+2\lambda+\mu, c+2\lambda+\mu, d+\lambda+\mu)$.
- (P'_6) The system (2.6) is invariant under re scaling of the variables and the parameters by $\nu > 0$, i.e. $x \mapsto \nu x$, $y \mapsto \nu y$ and $z \mapsto \nu z$, $a \mapsto \nu a$, $b \mapsto \nu b$, $c \mapsto \nu c$ and $d \mapsto \nu d$. If a, b, c and d are rational numbers, without loss of generality we can write them as

  $$a = \frac{p_1}{q}, \qquad b = \frac{p_2}{q}, \qquad c = \frac{p_3}{q}, \qquad \text{and} \quad d = \frac{p_4}{q}.$$

  Choosing $\nu = \frac{1}{q}$, we can transform the system into one with integer values parameter. This is also true when the parameters a, b, c and d are in e.g. $\eta\mathbb{Q} = \{s\eta \mid s \in \mathbb{Q}\}$ where η is an arbitrary but fixed irrational number.

3. General results of the system (2.6)

3.1. Proof that the integrals are functionally independent

If the integrals are functionally independent, by taking the intersection between the two-level sets generically we will find a one-dimensional piecewise-linear manifold in $\mathbb{R}^3$ which contains orbits. The two integral manifolds in our system consist of parallel plane segments. This means, there might be some open domains in $\mathbb{R}^3$ where we have plane segments as the intersection between the two-level sets. In those domains, the system (2.6) would have only one integral (instead of two) which implies that integrability is in question. For our system we prove that this is not the case.

Lemma 3.1. *The intersection between the integral manifolds is transversal almost everywhere. Hence, the integrals are functionally independent.*

Proof. The proof is done by inspection of all possible pairs of parallel plane segments constructing the two integral manifolds. We will work out two cases in detail and the rest can be done similarly.

Consider the plane $d + x + y + z = I_1^\circ$ and the plane $a - x - y - z = I_2^\circ$ which are parallel to each other. Suppose that the plane segment which corresponds to $d + x + y + z = I_1^\circ$ is present in the integral manifold $I_1 = I_1^\circ$. Then, for every point $(x_\circ, y_\circ, z_\circ)$ on that plane segment we have

$$d + x_\circ + y_\circ + z_\circ > \max(a + x_\circ, a + y_\circ, a + z_\circ, b + x_\circ + y_\circ, b + y_\circ + z_\circ, c + x_\circ + z_\circ),$$

provided $(x_\circ, y_\circ, z_\circ)$ is not on the boundary of the plane segment. Since

$$d + x_\circ + y_\circ + z_\circ > a + x_\circ,$$

it follows that

$$d - x_\circ > a - x_\circ - y_\circ - z_\circ.$$

As a consequence, the point $(x_\circ, y_\circ, z_\circ)$ is not on the plane segment: $a - x - y - z = I_2^\circ$ for all values of I_2°.

Let us now consider the plane segment $a + x = I_1^\circ$ and the plane segment $d - x = I_2^\circ$. Similarly, let $(x_\circ, y_\circ, z_\circ)$ be an arbitrary point satisfying $a + x_\circ = I_1^\circ$ which is not at the boundary. Then

$$a + x_\circ > \max(a + y_\circ, a + z_\circ, b + x_\circ + y_\circ, b + y_\circ + z_\circ, c + x_\circ + z_\circ, d + x_\circ + y_\circ + z_\circ).$$

From $a + x_\circ > d + x_\circ + y_\circ + z_\circ$ we conclude that: $a - x_\circ - y_\circ - z_\circ > d - x_\circ$. Thus the non-transversal intersection could occur only at the boundaries of each plane segment. By this we conclude that the intersection between I_1 and I_2 is transversal almost everywhere. □

Together with property (P_2'), lemma 3.1 implies that the system (2.6) is integrable.

3.2. The inverse mapping

Note that the integrals I_1 and I_2 are invariant under the transformation $x \mapsto z$ and $z \mapsto x$, which is the time-reversal symmetry. Applying this symmetry to the system (2.6), we obtain the mapping

$$\overline{x} = z + g(y, x), \qquad \overline{y} = x, \qquad \overline{z} = y. \tag{3.1}$$

It is easy to show that the above mapping is the inverse mapping of (2.6).

Lemma 3.2. *The system (2.6) defines a one-to-one mapping in $\mathbb{R}^3$ with the inverse mapping being (3.1).*

3.3. One-parameter family of fixed points

Let us now look for fixed points of the system (2.6). It is clear that fixed points are obtained by substituting $x = y = z$ into system (2.6). It turns out that the entire line $\{(x, y, z) = (s, s, s) \mid s \in \mathbb{R}\}$ consists of fixed points of the mapping (2.6) for all values of the parameters.

3.4. The existence of periodic solutions

Let us consider one of the level sets of I_1, i.e. $I_1(x, y, z) = I_1^\circ$ for some real constant number I_1°. From (2.7) we can immediately conclude that $x \leqslant I_1^\circ - a$, $y \leqslant I_1^\circ - a$ and $z \leqslant I_1^\circ - a$. Let us now look at the other level set, namely $I_2(x, y, z) = I_2^\circ$. We conclude similarly that $x \geqslant d - I_2^\circ$, $y \geqslant d - I_2^\circ$ and $z \geqslant d - I_2^\circ$.

Lemma 3.3. *The intersection between the two manifolds $I_1(x, y, z) = I_1^\circ$ and $I_2(x, y, z) = I_2^\circ$ lies inside the closed domain defined by a Cartesian product of three closed intervals, i.e.* $[d - I_2^\circ, I_1^\circ - a] \times [d - I_2^\circ, I_1^\circ - a] \times [d - I_2^\circ, I_1^\circ - a]$.

A consequence of lemma 3.3 for the dynamics of system (2.6) is interesting to note. Let us restrict ourselves for a moment to looking at integer values of the parameters. If we choose an initial condition $(x_1, y_1, z_1) \in \mathbb{Z}^3$, then for all natural numbers n, the solution of (2.6) corresponding to that initial condition satisfies $(x_n, y_n, z_n) \in \mathbb{Z}^3$. It should also lie on the intersection between the manifold $I_1 = I_1(x_1, y_1, z_1)$ and $I_2 = I_2(x_1, y_1, z_1)$, say $\mathcal{I}$. Since $\mathcal{I}$ lies inside the bounded box described in the above lemma, then $\mathcal{I} \cap \mathbb{Z}^3$ is a finite set of points.

Now let us consider the initial condition

$$\left(\frac{p_{11}}{q}, \frac{p_{21}}{q}, \frac{p_{31}}{q}\right) \in \mathbb{Q}^3.$$

The system (2.6) can be written as

$$\overline{x} = y, \qquad \overline{y} = z$$
$$\overline{z} = \frac{1}{q}\max(aq + qx, bq + qy + qx, cq + qz + qx, dq + qy + qz + qx) - \frac{1}{q}\max(aq, bq + qz, cq + qy, dq + qy + qz).$$

Thus, for all natural numbers n, the solution takes the form

$$\left(\frac{p_{1n}}{q}, \frac{p_{2n}}{q}, \frac{p_{3n}}{q}\right) \in \mathbb{Q}^3.$$

We conclude that the following holds.

Theorem 3.4. *If a, b, c and d are integers, a solution of (2.6) which starts at a rational point $(x_1, y_1, z_1) \in \mathbb{Q}^3$, is periodic.*

The above theorem provides us with the existence of periodic solutions in the system (2.6) if a, b, c and d are integers. In the view of property (P_6'), this existence of periodic solutions actually holds for a larger set of parameter values. Furthermore, there are actually uncountably many periodic solutions in the system (2.6). We will prove this in section 4.

4. Periodic and quasi-periodic solutions

Let us now fix a value for one of the integrals, say I_1. The level set $I_1 = C_1$ is a two-dimensional piecewise-linear surface in $\mathbb{R}^3$. We want to study the dynamics of the system (2.6) on the level set $I_1 = C_1$.

Lemma 4.1. *The dynamical system (2.6) restricted to the level set $I_1 = I_1^\circ$ is measure preserving.*

The idea of the proof for this lemma follows from the proof of theorem 1(ii) on p 2316 of [6]. The adaptation is done to include the situation where differentiability is only almost everywhere.

Proof. Let us write the mapping (2.6) as $\overline{\boldsymbol{\xi}} = \Phi(\boldsymbol{\xi})$. Since (2.6) is volume preserving, then

$$\int_U \mathrm{d}\boldsymbol{\xi} = \int_{\Phi(U)} \mathrm{d}\overline{\boldsymbol{\xi}},$$

for all $U \subset \mathbb{R}^3$. Let us take a volume element V which has arbitrary projection on the integral manifold $I_1 = I_1^\circ$. Since the integral manifold is piecewise linear, then $V = \cup_{j\in J} V_j$ while the projection of V_j is called A_j. Let $\boldsymbol{\alpha}_j = (\alpha_1, \alpha_2)_j$ be the coordinates in A_j while t_j is the coordinate orthogonal to A_j. Then

$$\int_V \mathrm{d}\boldsymbol{\xi} = \sum_{j\in J} \int_{V_j} \frac{\partial \boldsymbol{\xi}}{\partial(\boldsymbol{\alpha}_j, t_j)}\, \mathrm{d}\boldsymbol{\alpha}_j\, \mathrm{d}t_j,$$

where $J = \{1, 2, \ldots, n\}$. Note that the derivatives are now well defined on each V_j. We do the same for $\Phi(V)$, and then taking all the $\mathrm{d}t_j \to 0$, we have

$$\sum_{j\in J} \int_{A_j} \left.\frac{\partial \boldsymbol{\xi}}{\partial(\boldsymbol{\alpha}_j, t_j)}\right|_{t_j=0} \mathrm{d}\boldsymbol{\alpha}_j = \sum_{j\in J'} \int_{\overline{A_j}} \left.\frac{\partial \boldsymbol{\xi}}{\partial(\overline{\boldsymbol{\alpha}_j}, \overline{t_j})}\right|_{\overline{t_j}=0} \mathrm{d}\overline{\boldsymbol{\alpha}_j},$$

which completes the proof. □

For arbitrary values of the second integral I_2 (greater than a certain bound which will be determined later), the intersection between the two-level sets gives us a polygon-like shape on the piecewise-linear surface defined by $I_1 = I_1^\circ$. We have the following theorem.

Theorem 4.2. *Let P be the intersection between $I_1 = I_1^\circ$ and $I_2 = I_2^\circ$. We assume that P contains a T-periodic solution with $T \in \mathbb{N}$, i.e.*

$$\{\boldsymbol{\xi}_n = (x_n, y_n, z_n) \mid n = 0, 1, \ldots, T-1\}.$$

Then, every point in P is a T-periodic point of the mapping (2.6).

Proof. Let us define $\varphi_T : \mathbb{R}^3 \to \mathbb{R}^3$ which is the Tth iterate of the mapping (2.6). Then $\boldsymbol{\xi}_n, n = 0, 1, \ldots, T-1$, are fixed points of the mapping φ_T. Let us assume that the part of polygon P which connects $\boldsymbol{\xi}_0$ and $\boldsymbol{\xi}_1$ consists of two line-segments L_1 and L_2. Let us call the point where the two segments join $\boldsymbol{\xi}_{\frac{1}{2}}$. Then L_1 can be written as

$$\boldsymbol{\xi} = \boldsymbol{\xi}_0 + 2t\big(\boldsymbol{\xi}_{\frac{1}{2}} - \boldsymbol{\xi}_0\big), \qquad t \in \big[0, \tfrac{1}{2}\big), \tag{4.1}$$

while L_2 can be written as

$$\boldsymbol{\xi} = \boldsymbol{\xi}_{\frac{1}{2}} + 2\big(t - \tfrac{1}{2}\big)\big(\boldsymbol{\xi}_1 - \boldsymbol{\xi}_{\frac{1}{2}}\big), \qquad t \in \big[\tfrac{1}{2}, 1\big]. \tag{4.2}$$

The two relations in (4.1) and (4.2) define a mapping $\phi : [0, 1] \to L_1 \cup L_2$. Moreover, the mapping is one to one and thus, invertible. By doing this, we have associated the mapping $\varphi_T : \mathbb{R}^3 \to \mathbb{R}^3$ with a mapping $\phi^{-1} \circ \varphi_T \circ \phi : [0, 1] \to [0, 1]$, which is also, one to one and piecewise linear. The construction of ϕ is naturally extended to the case where the part of P connecting $\boldsymbol{\xi}_0$ and $\boldsymbol{\xi}_1$ consists of a larger but finite number of line segments.

Note that, for $t \in (0, 1)$ either $\phi^{-1} \circ \varphi_T \circ \phi(t) - t \geqslant 0$ or $\phi^{-1} \circ \varphi_T \circ \phi(t) - t \leqslant 0$. In the first case, if $\phi^{-1} \circ \varphi_T \circ \phi(t) - t > 0$ for all t, then $t = 1$ is an asymptotically stable (attracting) fixed point. This is a violation of the measure preserving nature of the mapping (2.6). Thus we have $(\phi^{-1} \circ \varphi_T \circ \phi)(t) = t$ for all $t \in (0, 1)$. The second case can be treated similarly. □

The following corollaries can be proven using similar methods with the proof of theorem (4.2).

Corollary 4.3. *Every solution on the polygon P containing a non-periodic point is quasi-periodic. The polygon P is densely filled by the orbit of any of those solutions.*

Corollary 4.4. *The integral manifold $I_1 = I_1^\circ$ is fibred by polygons (which are parametrized by the value of the second integral $I_2 = I_2^\circ$) on which either periodic or quasi-periodic motions take place.*

5. The integral manifolds

In general, both of the integral manifolds consist of at least three and at most seven plane segments. The number of plane segments in each integral manifold is obviously dependent on the value of the parameters. In an integrable system, such as ours, it is natural to use the value of the integrals as parameters in the system. In this paper, we will restrict the dynamics to one-level set of I_1, namely $I_1 = I_1^\circ$. The results would be the same if one would have chosen to fix I_2 instead.

There are eight possibilities for the shape of the integral manifold $I_1 = I_1^\circ$. For convenience, we name the planes constructing the integral manifold in the following definition.

Definition 5.1. *The plane segments in the integral manifold corresponding to $x + y + b = I_1^\circ$ and $y + z + b = I_1^\circ$ are called the B-planes. The plane segment corresponding to $c + x + z = I_1^\circ$ is the* C*-plane. The plane segment corresponding to $d + x + y + z = I_1^\circ$ is the* D*-plane, and the plane segments corresponding to $x + a = I_1^\circ$, $y + a = I_1^\circ$ and $z + a = I_1^\circ$ are called the A-planes.*

In figure 1, we have drawn all possible shapes of the integral manifolds $I_1 = I_1^\circ$. Depending on the parameters, we may have different scenarios of shape changes as we vary the value of I_1.

Lemma 5.2. *Consider the integral manifold $I_1 = I_1^\circ$.*

(1) The plane segment corresponding to $c + x + z = I_1^\circ$ does not appear in the integral manifold $I_1 = I_1^\circ$ if and only if $2a - c \geqslant I_1^\circ$.
(2) The plane segments corresponding to $b + x + y = I_1^\circ$ and to $b + y + z = I_1^\circ$ do not appear in the integral manifold $I_1 = I_1^\circ$ if and only if $2a - b \geqslant I_1^\circ$.
(3) The plane segment corresponding to $d + x + y + z = I_1^\circ$ does not appear in the integral manifold $I_1 = I_1^\circ$ if and only if $2b + c - 2d \geqslant I_1^\circ$ or $\frac{1}{2}(3a - d) \geqslant I_1^\circ$.

Proof. (1) From (2.7) it follows that $x + a \leqslant I_1^\circ$. Then

$$\begin{aligned} x + z + c &\leqslant z + I_1^\circ - a + c \\ &\leqslant z + a + (I_1^\circ - 2a + c). \end{aligned}$$

Thus, if $(2a - c) \geqslant I_1^\circ$ the plane segment corresponding to $c + x + z = I_1^\circ$ does not appear in the integral manifold $I_1 = I_1^\circ$. Consider the situation where $(2a - c) < I_1^\circ$ which implies that $I_1^\circ = (2a - c) + q^2$ (for some q). Consider the following set of inequalities:

$$x + a \leqslant (2a - c) + q^2 \tag{5.1}$$

$$y + a \leqslant (2a - c) + q^2 \tag{5.2}$$

$$z + a \leqslant (2a - c) + q^2 \tag{5.3}$$

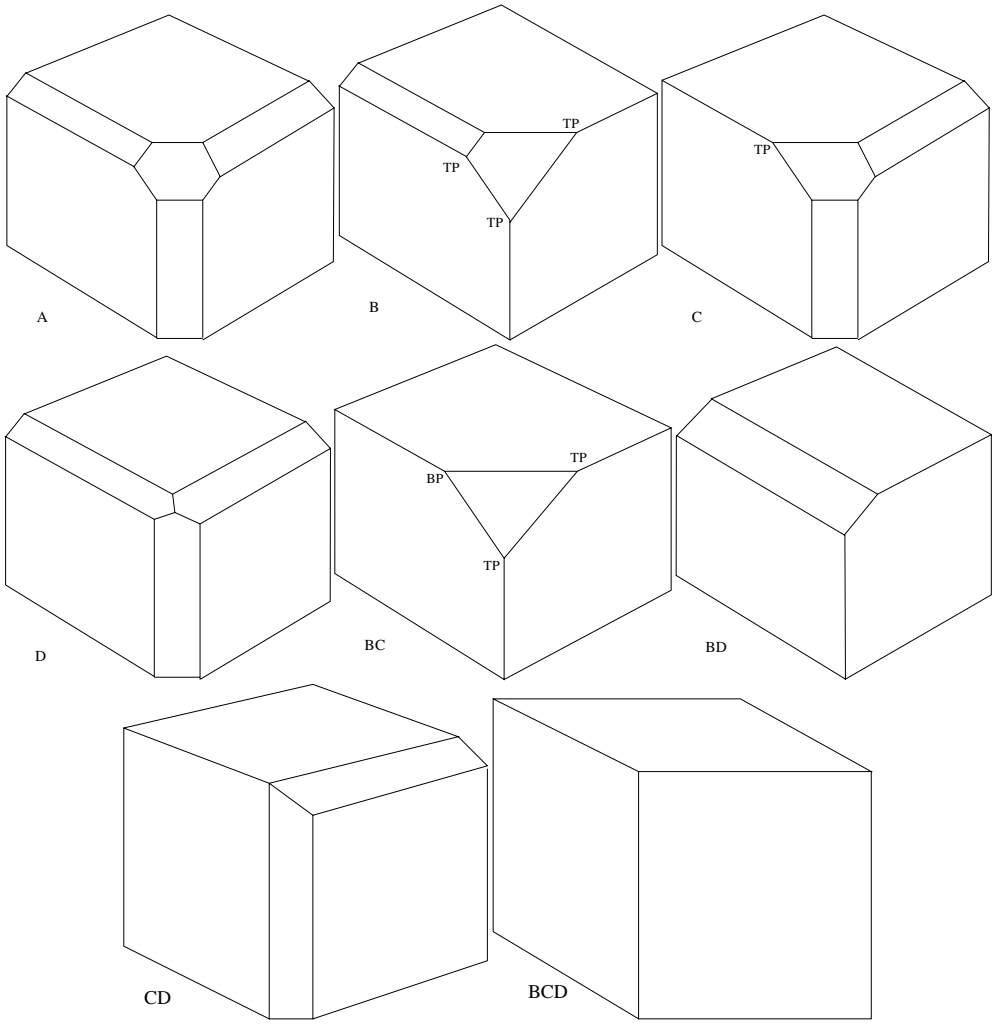

Figure 1. In this figure we have drawn all possible shape of the integral manifold $I_1 = I_1^{\circ}$. From the left to right, top to bottom, we have the situation where we have all seven planes, no B-planes, no C-plane, no D-plane, no B- and C-planes, no B- and D-planes, no C- and D-planes and no B-, C- and D-planes. See definition 5.1 for definition of the planes.

$$x + y + b \leqslant (2a - c) + q^2 \tag{5.4}$$

$$y + z + b \leqslant (2a - c) + q^2 \tag{5.5}$$

$$x + z + c \leqslant (2a - c) + q^2 \tag{5.6}$$

$$x + y + z + d \leqslant (2a - c) + q^2. \tag{5.7}$$

We will show that there exists a solution $(x_\circ, y_\circ, z_\circ)$ of the system above, which satisfies $x_\circ + z_\circ + c = (2a - c) + q^2$ or, equivalently, $z_\circ = 2\,(a - c) + q^2 - x_\circ$. From inequality (5.3) we have $(a - c) \leqslant x_\circ$. Together with inequality (5.1), we have

$$(a - c) \leqslant x_\circ \leqslant (a - c) + q^2.$$

Finally, we choose

$$y_\circ \leqslant \min(c - d + q^2, a - b + q^2, a - c + q^2),$$

which concludes the proof of (1).
(2) This is proved by a similar technique to (1).
(3) Let us now consider the three planes: $x + z = I_1^\circ - c$, $y + z = I_1^\circ - b$ and $x + y = I_1^\circ - b$. The three planes intersect each other at the point

$$(x_\circ, y_\circ, z_\circ) = \left(\tfrac{1}{2}(I_1^\circ - c), \tfrac{1}{2}(I_1^\circ + c - 2b), \tfrac{1}{2}(I_1^\circ - c)\right).$$

Thus, by requiring that $x_\circ + y_\circ + z_\circ + d - I_1^\circ \leqslant 0$, we conclude that $x + y + z + d \leqslant \max(x + z + c, y + z + b, x + y + b)$ if $2b + c - 2d \geqslant I_1^\circ$. Let us also consider the planes $x = I_1^\circ - a$, $y = I_1^\circ - a$ and $z = I_1^\circ - a$. The intersection between the three planes is $(I_1^\circ - a, I_1^\circ - a, I_1^\circ - a)$. Similar to the previous analysis, we conclude that $x + y + z + d \leqslant \max(x + a, y + a, z + a)$ if $\frac{1}{2}(3a - d) \geqslant I_1^\circ$. □

For the other integral manifold, i.e. $I_2 = I_2^\circ$, similar results as in lemma 5.2 can be derived. The proof is omitted since it is identical to the proof of lemma 5.2.

Lemma 5.3. *Consider the integral manifold $I_2 = I_2^\circ$.*

(1) The plane segment corresponding to $c - x - z = I_2^\circ$ does not appear in the integral manifold $I_2 = I_2^\circ$ if and only if $2d - c \geqslant I_2^\circ$.
(2) The plane segments corresponding to $b - x - y = I_2^\circ$ and to $b - y - z = I_2^\circ$ do not appear in the integral manifold $I_2 = I_2^\circ$ if and only if $2d - b \geqslant I_2^\circ$.
(3) The plane segment corresponding to $a - x - y - z = I_2^\circ$ does not appear in the integral manifold $I_2 = I_2^\circ$ if and only if $2b + c - 2a \geqslant I_2^\circ$ or $\frac{1}{2}(3d - a) \geqslant I_2^\circ$.

From lemma 5.2 we know that there are four numbers on the real line: $\theta_1 = 2a - c, \theta_2 = 2a - b, \theta_3 = 2b + c - 2d$ and $\theta_4 = \frac{1}{2}(3a - d)$ which are important in the shape changes of the integral manifold $I_1 = I_1^\circ$. Note that

$$\frac{\theta_1 + 2\theta_2 + \theta_3}{4} = \theta_4,$$

which implies that we can only choose three out of the four θ arbitrarily. Moreover, from the above relation one can see that θ_4 is located at the mid-point of the average between θ_1 and θ_3, i.e. $\frac{\theta_1 + \theta_3}{2}$ and θ_2.

5.1. Topological change of the integral manifold $I_1 = I_1^\circ$

In table 1, we have presented all possible scenarios for the topological changes in the integral manifold $I_1 = I_1^\circ$. In general, for large enough value of I_1° the integral manifold contains all seven plane segments. In figure 1 this situation is drawn as shape A. For small enough value of $I_1 = I_1^\circ$, the integral manifold contains three plane segments corresponding to shape BCD in figure 1.

Let us consider, as an example, the first row on table 1. On the third column, we have put the sequence of shapes of the integral manifold $I_1 = I_1^\circ$. For a large value of I_1° namely $I_1^\circ > \theta_3$, as mentioned earlier, we have all seven planes present in the integral manifold. This corresponds to shape A in figure 1. As we decrease the value of I_1° so that $\theta_1 < I_1^\circ < \theta_3$, we move to the situation where the D-plane disappears. If $\theta_4 < I_1^\circ < \theta_1$, then the C-plane disappears. Thus, we have the CD shape as is drawn in figure 1. No topological change occurs as we pass the value of θ_4. Finally, as we pass the value of θ_2 the B-plane disappears.

Table 1. In this table we have presented all possible scenarios for shape transitions as we vary the value of I_1. Although the arrow is pointing to the right, actually it is easier to read in the other direction. Take for example the row number one. We start with a value of $I_1^\circ > \theta_3$. Passing θ_3, the integral manifold $I_1 = I_1^\circ$ changes from having shape A to shape D (see figure 1 for the shapes). Then, crossing θ_1, the shape changes from shape D to shape CD, and so forth.

No.	Assumption	Condition	Sequence of shapes
1	$\theta_1 < \theta_3$	$\theta_2 < \theta_4 < \theta_1 < \theta_3$	BCD → CD → CD → D → A
2		$\theta_2 < \theta_4 = \theta_1 < \theta_3$	BCD → CD → D → A
3		$\theta_2 < \theta_1 < \theta_4 < \theta_3$	BCD → CD → D → D → A
4		$\theta_1 < \theta_2 < \theta_4 < \theta_3$	BCD → BD → D → D → A
5		$\theta_1 < \theta_2 = \theta_4 < \theta_3$	BCD → BD → D → A
6		$\theta_1 < \theta_4 < \theta_2 < \theta_3$	BCD → BD → BD → D → A
7		$\theta_1 < \theta_4 < \theta_2 = \theta_3$	BCD → BD → BD → A
8		$\theta_1 < \theta_4 < \theta_3 < \theta_2$	BCD → BD → BD → B → A
9		$\theta_1 < \theta_4 = \theta_3 < \theta_2$	BCD → BD → B → A
10		$\theta_1 < \theta_3 < \theta_4 < \theta_2$	BCD → BD → BD → B → A
11	$\theta_1 > \theta_3$	$\theta_2 < \theta_4 < \theta_3 < \theta_1$	BCD → CD → CD → C → A
12		$\theta_2 < \theta_4 = \theta_3 < \theta_1$	BCD → CD → C → A
13		$\theta_2 < \theta_3 < \theta_4 < \theta_1$	BCD → CD → CD → C → A
14		$\theta_2 = \theta_3 < \theta_4 < \theta_1$	BCD → CD → C → A
15		$\theta_3 < \theta_2 < \theta_4 < \theta_1$	BCD → CD → CD → C → A
16		$\theta_3 < \theta_2 = \theta_4 < \theta_1$	BCD → BCD → C → A
17		$\theta_3 < \theta_4 < \theta_2 < \theta_1$	BCD → BCD → BC → C → A
18		$\theta_3 < \theta_4 < \theta_1 < \theta_2$	BCD → BCD → BC → B → A
19		$\theta_3 < \theta_4 = \theta_1 < \theta_2$	BCD → BCD → B → A
20		$\theta_3 < \theta_1 < \theta_4 < \theta_2$	BCD → BCD → BD → B → A
21	$\theta_1 = \theta_3$	$\theta_2 < \theta_4 < \theta_1$	BCD → CD → CD → A
22		$\theta_1 < \theta_4 < \theta_2$	BCD → BD → B → A

Let us write $\theta_5 = 2d - c$, $\theta_6 = 2d - b$, $\theta_7 = 2b + c - 2a$ and $\theta_8 = \frac{1}{2}(3d - a)$. Here we also find a relation which is similar to the relation between $\theta_1, \theta_2, \theta_3$ and θ_4, i.e.

$$\frac{\theta_5 + 2\theta_6 + \theta_7}{4} = \theta_8.$$

Moreover, we find that

$$\theta_{j+1} - \theta_1 = \theta_{j+5} - \theta_5, \quad j = 1, 2, 3.$$

Remark 5.4. Using the fact that the relative distance between the bifurcation points are the same, we could define a shift on the integrals by

$$\tilde{I}_1 = I_1 - 2a, \qquad \text{and} \qquad \tilde{I}_2 = I_2 - 2d,$$

which implies that

$$\theta_1 = -c = \theta_5, \qquad \theta_2 = -b = \theta_6, \qquad \theta_3 = 2b + c - 2a - 2d = \theta_7,$$

and

$$\theta_4 = -\tfrac{1}{2}(a + d) = \theta_8.$$

This would quantitatively simplify the analysis.

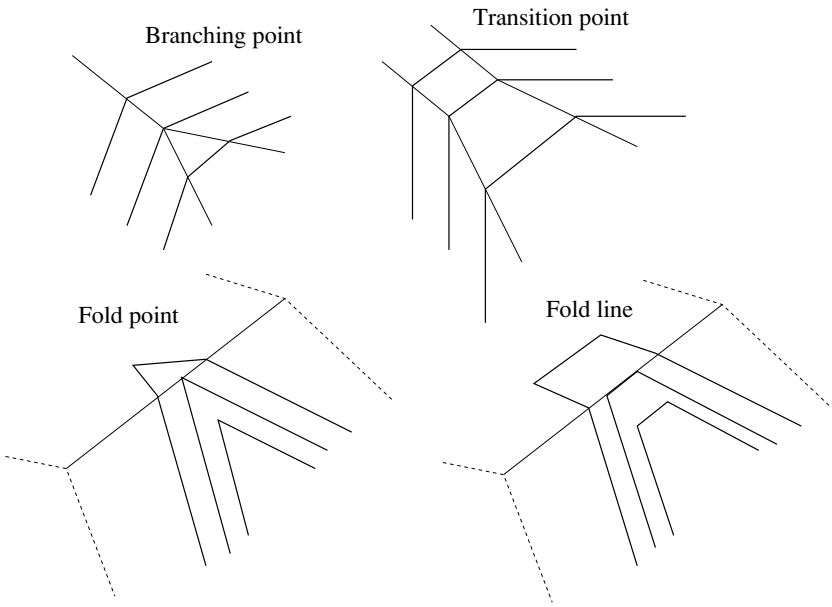

Figure 2. In this figure, we have drawn possible bifurcations scenarios due to the non-smoothness of the integral manifold $I_1 = I_1^\circ$. The branching point is that where the polygon gets an extra side as it passes the point. The transition point is the situation where the polygon changes side. The fold point is losing two sides due to the fact that the integral manifold is folded. The fold line is similar to the fold point.

6. Topological changes of the polygons

In this section we will describe the topological changes of the polygons containing the solutions of (2.6). There are two sources for these topological changes:

(S_1) the non-smoothness of the integral manifold $I_1 = I_1^\circ$, and

(S_2) the fact that plane segments can disappear from the integral manifold $I_2 = I_2^\circ$ as we vary the value of I_2°.

After fixing the integral manifold $I_1 = I_1^\circ$, we will be in one of the situations drawn in figure 1. There are at least four possibilities of topological changes of the polygons, i.e. the *branching point*, the *transition point*, the *fold point* and the *fold line*. If three plane segments in the integral manifold intersect at a point, we call that point the branching point. In the neighbourhood of the branching point, the polygon gets an extra side (or loses one side). The second situation is when two plane segments intersect at a line on the integral manifold, and the line happens to be parallel to one of the edges of the polygon. In this situation the polygon does not get an extra side.

The others are the situations where two plane segments intersect at a line L on the integral manifold. Moreover, there exist two intersection points $\boldsymbol{p}_1$ and $\boldsymbol{p}_2$ between the polygon and L. As we vary the value of the other integral, the polygon moves towards L. As a consequence, $|\boldsymbol{p}_1 - \boldsymbol{p}_2|$ might go to zero or to a finite nonzero number. In the case the distance goes to zero we call it fold point while the other is fold line. We illustrate these two situation in figure 2.

A different topological change of the polygon is due to the topological changes in the integral manifold as we vary the value of the integral. For instance, using lemma 5.2, we

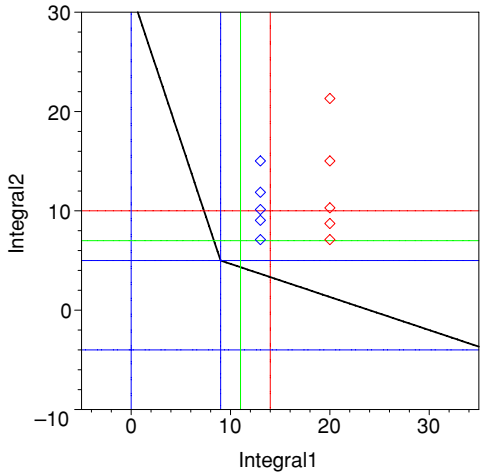

Figure 3. In this figure we have plotted the two-parameter 'bifurcation' diagram. On the horizontal axis is the value of the integral I_1 while in the vertical is I_2. The red lines are $I_1 = 14$ and $I_2 = 10$. The green lines are $I_1 = 11$ and $I_2 = 7$, while the blue lines are $I_1 = 9, I_1 = 0, I_2 = 5$ and $I_2 = -4$. The thickened line is the lower bound for the value of I_2. This is obtained by computing the value of I_2 at the fixed point. In this figure we have drawn some points using red diamonds and blue diamonds. The red diamonds represent the initial values taken in figure 4 while the blue diamonds are for figure 5.

can distinguish several possible transitions of the shape of I_1, which are presented in table 1. Similar results can be derived for the other integral manifold by using lemma 5.3.

We would like to note that although the topological shape of the integral manifold $I_2 = I_2^\circ$ changes as we vary the value of I_2°, the topological shape of the polygon may not be affected. In the following section, we will describe an example where this happens.

We proceed with the bifurcation analysis of system (2.6) as follows. First, we fix the values of the parameters a, b, c and d. For that chosen combination, we look at the first column of table 1 to determine in which situation we are. Then, we fix a value for I_1 namely $I_1 = I_1^\circ$, and by this we fix a shape for it. In that integral manifold, we are looking for possible branching points, transition points, fold points or fold lines. This is done by looking for intersection between plane segments in the integral manifold.

Next, we will choose initial conditions such that they all lie on the integral manifold $I_1 = I_1^\circ$. We will also keep track of the value of I_2 on each of the initial conditions and compare it with the similar table as in table 1, but derived from lemma 5.3.

7. An example

In this section we have taken the parameters to be $a = 8, b = 5, c = 2$ and $d = 6$. For this choice of the parameters' values, $\theta_1 = 14, \theta_2 = 11, \theta_3 = 0, \theta_4 = 9, \theta_5 = 10, \theta_6 = 7, \theta_7 = -4$ and $\theta_8 = 5$. Thus $\theta_3 < \theta_4 < \theta_2 < \theta_1$, which is the 18th row in table 1.

In figure 3 we have drawn the lines: $I_1 = \theta_j$ and $I_2 = \theta_{j+4}$, $j = 1, 2, 3, 4$. Recall that these lines are the lines where the integral manifolds $I_1 = I_1^\circ$ and $I_2 = I_2^\circ$ undergo topological changes. The red lines are $I_1 = \theta_1$ and $I_2 = \theta_5$. Going from right to left with I_1°, the plane segment which corresponds to $c + x + z = I_1^\circ$ disappears from the integral manifold as we pass $I_1 = \theta_1$. Similarly by going down with I_2°, the plane segment which corresponds to $c - x - z = I_2^\circ$ disappears from $I_2 = I_2^\circ$ as we pass $I_2 = \theta_5$. The green lines are $I_1 = \theta_2$

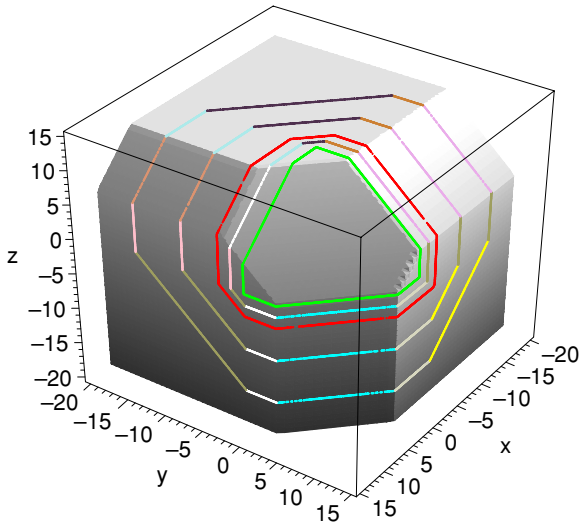

Figure 4. In this figure we draw the situation where $I_1^\circ = 20 > \theta_1 = 14$. The integral manifold $I_1 = I_1^\circ$ has seven plane segments. For several initial conditions we draw the orbits of (2.6). These orbits correspond to the red diamonds in figure 3. The outermost one corresponds to the highest red diamond in figure 3. The red polygon represents a polygon which is close to the critical polygon. This corresponds to the horizontal red line in figure 3. Similarly, the green polygon corresponds to the green line in figure 3.

and $I_2 = \theta_6$, and they correspond to the vanishing of the plane segments corresponding to $b + x + y = I_1^\circ$, $b + y + z = I_1^\circ$, $b - x - y = I_2^\circ$ and $b - y - z = I_2^\circ$. The blue lines are for vanishing of the plane segments corresponding to $d + x + y + z = I_1^\circ$ and $a - x - y - z = I_2^\circ$.

It is clear that as we fix the value of I_1, by decreasing the value of I_2, the polygon containing the solutions gets smaller. At a certain value, the polygon collapses into the fixed point. This defines an equation relating I_1 with I_2. The graph of this equation is drawn in figure 3 using the thickened line. Below this line, we have no solution for the system (2.6).

7.1. The case where $I_1^\circ = 20$

Let us now look at figure 4 in where we have drawn the integral manifold $I_1^\circ = 20$. One can easily see that at this value, $I_1^\circ > \theta_1$, which implies that the integral manifold consists of seven plane segments. On this integral manifold we have chosen six initial conditions and drawn the orbits on the same plot. Note that these initial conditions are chosen such that they are all lying on the integral manifold $I_1^\circ = 20$. This is done for example by choosing arbitrary x and y and solve for z the equation $I_1^\circ = 20$. Moreover, due to theorem 4.2, x and y have to be chosen so that they lie on a non-periodic polygon. These initial conditions can also be represented by the value of the second integral, i.e. from the outermost one: $I_2^\circ = 21.31\ldots, 15.02\ldots, 10.30\ldots, 8.73\ldots$ and $7.10\ldots$.

As we approach the red line $I_2^\circ = \theta_5 = 10$ in figure 3, the part of the polygon on the plane $y =$ constant which is coloured yellow, is getting smaller. Recall that in figure 3, the line $I_2^\circ = \theta_5$ represents the vanishing of the plane segment $c - x - z = I_2^\circ$. The orbit for $I_2^\circ = 10.30\ldots$ is drawn using the red colour. This orbit is on a polygon which is close to a critical polygon where the integral manifold of I_2 loses its C-plane. As a consequence, the yellow part of the polygon vanishes.

Another topological change occurs as I_2 approaches $\theta_6 = 7$. This time, the line coloured black on the $z =$ const plane, and the line coloured khaki on the $x =$ const plane vanish. The critical polygon is coloured green. Recall that θ_6 corresponds to the vanishing of the two B-planes from the integral manifold of I_2.

The red polygon is also the critical polygon in which we have a transition point (see section 2 for a definition). One can see that the orbit outside the red polygon has one side which is coloured orange. After passing the red polygon, the side changes colour to white. The length of that white side is larger than the orange side. Another transition point occurs at the critical polygon which is coloured green.

7.1.1. Period-three dynamics. Let P_g be the domain on the manifold $I_1 = 20$ which is bounded by the green polygon. Let us take an arbitrary initial condition in P_g. Then the solution (x_n, y_n, z_n) of the system (2.6) is in P_g for all n. Recall that

$$I_1 = \max(a + x, a + y, a + z, b + x + y, b + y + z, c + x + z, d + x + y + z),$$

and

$$I_2 = \max(d - x, d - y, d - z, b - y - z, b - x - y, c - x - z, a - x - y - z).$$

The geometry of P_g implies that

$$\max(a + x, a + y, a + z, d + x + y + z) = I_1. \tag{7.1}$$

Moreover, since $I_2 < \theta_6 = 2d - b$, then the integral manifold I_2 has lost its B-planes and C-plane. It implies that

$$\max(d - x, d - y, d - z, a - x - y - z) = I_2 < 2d - b. \tag{7.2}$$

Note that (7.2) implies that $x > b - d$, $y > b - d$ and $z > b - d$.

Let us now pay attention to the function $g(y, z) = \max(a, b + y, c + z, d + y + z) - \max(a, b + z, c + y, d + y + z)$. Suppose that there exists a point $(x_\circ, y_\circ, z_\circ) \in P_g$ such that $b + y_\circ \geqslant \max(a, c + z_\circ, d + y_\circ + z_\circ)$. Then $b + y_\circ \geqslant d + y_\circ + z_\circ$ which is a contradiction. It means that $b + y < \max(a, b + y, c + z, d + y + z)$ for all point in P_g.

Note that $2d - c = \theta_5 > \theta_6 = 2d - b$ which is equivalent to $c < b$. Suppose that there exists a point $(x_\circ, y_\circ, z_\circ) \in P_g$ such that $c + z_\circ \geqslant \max(a, b + y_\circ, d + y_\circ + z_\circ)$. Then $c + z_\circ \geqslant d + y_\circ + z_\circ$, which implies $c - d \geqslant y_\circ$. But $b - d > c - d \geqslant y_\circ$ which is a contradiction.

By using similar methods, we can show that $b + z$ and $c + y$ cannot be the maximum of $\{a, b + z, c + y, d + y + z\}$. This implies that for all $(x, y, z) \in P_g$, $g(y, z) = 0$. Thus, *every point in P_g is a period-three point*. This is also true for $I_1 \leqslant 11 = \theta_2$ (the left side of the vertical green line in figure 3).

7.2. The case where $I_1 = 13$

Let us pay attention to the $y =$ const plane. Recall that for $I_1 = 20$ we have the phenomenon of a vanishing side in this plane. This phenomenon occurs as the polygon passes through the red polygon in figure 4. The side which vanishes is coloured yellow.

In figure 5, the corresponding side is coloured gold. The colour is different since it corresponds to a different intersection between plane segments of the integral manifolds. The one which is coloured yellow in figure 4 is the intersection between the $y =$ const plane of I_1 with the C-plane of I_2. That is why that side vanishes as I_2 passes θ_5. The side which is coloured gold in figure 5 is the intersection between the $y =$ const plane of I_1 with the A-plane of I_2. That is why we do not see this side vanishing as I_2 passes θ_5.

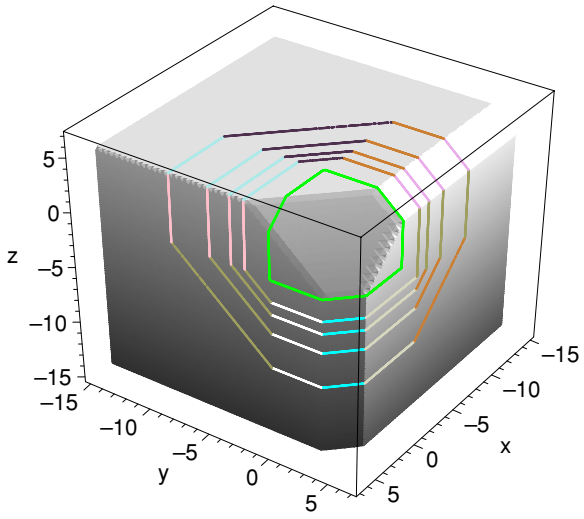

Figure 5. In this figure we draw the situation where $I_1^\circ = 13$. The integral manifold $I_1 = I_1^\circ$ has already lost its C-plane segments. For several initial conditions we draw the orbits of (2.6). These orbits correspond to the blue diamonds in figure 3. The outermost one corresponds to the highest blue diamond in figure 3. The green polygon corresponds to the green line in figure 3.

Passing through $I_2 = 9.04\ldots$, the polygon goes thourgh a branching point where the polygon gets an extra side. At the green coloured critical polygon, there is also the transition point behaviour. Just as in the previous case, every point inside the green polygon is a period-three point.

8. Concluding remarks

We have described the dynamics of the three-dimensional piecewise-linear integrable mapping (2.6). Each level set of I_1 is fibred by invariant polygons which are the intersections between the level sets of I_1 and I_2 for various initial conditions. On each polygon, the motion is either periodic or quasi-periodic.

Acknowledgments

The present work on three-dimensional integrable piecewise-linear systems has been inspired by Jim Scully's unpublished thesis on the two-dimensional case. We gratefully acknowledge financial support from the Australian Research Council Centre of Excellence for Mathematics and Statistics of Complex Systems. JMT thanks Santi Goenarso for her support in various ways. KMT thanks Professor G R W Quispel for the invitation and warm hospitatility.

Appendix A. General settings

Consider $\mathbb{R}^3$ with coordinates (u, v, w). We define a dynamical system on $\mathbb{R}^3$ by considering a mapping given by

$$\overline{u} = v, \qquad \overline{v} = w, \qquad \overline{w} = uf(v, w), \tag{A.1}$$

where $f : \mathbb{R}^2 \to \mathbb{R}$. We assume that there exists a function $H : \mathbb{R}^3 \to \mathbb{R}$ such that

$$H(\overline{u}, \overline{v}, \overline{w}) = H(u, v, w).$$

Such a function is called an integral of the system (A.1).

Let us now transform the variables by

$$u = \exp\left(\frac{x}{\varepsilon}\right), \qquad v = \exp\left(\frac{y}{\varepsilon}\right), \qquad w = \exp\left(\frac{z}{\varepsilon}\right), \tag{A.2}$$

with a view to taking the limit $\varepsilon \to 0$ later on. We need to transform also the parameters involved in the system but at the moment we are not concerned about this. The transformations (A.2) were first introduced by Tokihiro *et al* [8]. For the purpose of the transformation, we assume that all of our variables and parameters are positive. We remark that recently, the work of Ochiai [1] provides us with the opportunity to treat systems which involve subtraction.

Applying the transformation to (A.1) and then taking the limit of ε goes to zero, leads to

$$\overline{x} = y, \qquad \overline{y} = z, \qquad \overline{z} = x + g(y, z), \tag{A.3}$$

where

$$g(y, z) = \lim_{\varepsilon \to 0} \varepsilon \ln\left(f\left(\exp\left(\frac{y}{\varepsilon}\right), \exp\left(\frac{z}{\varepsilon}\right)\right)\right),$$

provided the limit exists.

Let us now define the function $K : \mathbb{R}^3 \to \mathbb{R}$, by

$$K(x, y, z) = \lim_{\varepsilon \to 0} \varepsilon \ln\left(H\left(\exp\left(\frac{x}{\varepsilon}\right), \exp\left(\frac{y}{\varepsilon}\right), \exp\left(\frac{z}{\varepsilon}\right)\right)\right), \tag{A.4}$$

assuming the limit exists. We have the following theorem.

Theorem A.1. *The function (A.4) is an integral of the system (A.3).*

Proof. Using the transformation, we let

$$u = \exp\left(\frac{x}{\varepsilon}\right), \qquad v = \exp\left(\frac{y}{\varepsilon}\right), \qquad w = \exp\left(\frac{z}{\varepsilon}\right),$$
$$\overline{u} = \exp\left(\frac{\overline{x}}{\varepsilon}\right), \qquad \overline{v} = \exp\left(\frac{\overline{y}}{\varepsilon}\right), \qquad \text{and} \quad \overline{w} = \exp\left(\frac{\overline{z}}{\varepsilon}\right).$$

Consider $\overline{w} = uf(v, w)$, or equivalently

$$\begin{aligned}\overline{w} &= \exp\left(\frac{x}{\varepsilon}\right) f\left(\exp\left(\frac{y}{\varepsilon}\right), \exp\left(\frac{z}{\varepsilon}\right)\right) \\ &= \exp\left(\frac{x + \varepsilon \ln f\left(\exp\left(\frac{y}{\varepsilon}\right), \exp\left(\frac{z}{\varepsilon}\right)\right)}{\varepsilon}\right).\end{aligned}$$

By definition we have (assuming the limit exists):

$$\begin{aligned}K(x, y, z) &= \lim_{\varepsilon \to 0} \varepsilon \ln\left(H\left(\exp\left(\frac{x}{\varepsilon}\right), \exp\left(\frac{y}{\varepsilon}\right), \exp\left(\frac{z}{\varepsilon}\right)\right)\right) \\ &= \lim_{\varepsilon \to 0} \varepsilon \ln\left(H\left(u, v, w\right)\right) \\ &= \lim_{\varepsilon \to 0} \varepsilon \ln\left(H\left(\overline{u}, \overline{v}, \overline{w}\right)\right) \text{ since } H \text{ is an integral of (A.1)} \\ &= \lim_{\varepsilon \to 0} \varepsilon \ln\left(H\left(v, w, \exp\left(\frac{x + \varepsilon \ln f\left(\exp\left(\frac{y}{\varepsilon}\right), \exp\left(\frac{z}{\varepsilon}\right)\right)}{\varepsilon}\right)\right)\right).\end{aligned}$$

We have assumed the existence of the following limit:

$$\lim_{\varepsilon \to 0} \varepsilon \ln f\left(\exp\left(\frac{y}{\varepsilon}\right), \exp\left(\frac{z}{\varepsilon}\right)\right) = g(y, z).$$

This implies that

$$K(x, y, z) = \lim_{\varepsilon \to 0} \varepsilon \ln \left(H \left(\exp\left(\frac{y}{\varepsilon}\right), \exp\left(\frac{z}{\varepsilon}\right), \exp\left(\frac{x + g(y, z)}{\varepsilon}\right)\right)\right),$$
$$= K(\overline{x}, \overline{y}, \overline{z}),$$

which completes the proof. □

Appendix B. Remark on the volume preservation property

Consider a general mapping:

$$\overline{u} = v, \qquad \overline{v} = w, \qquad \overline{w} = F(u, v, w),$$

where there exists a measure density function $m(u, v, w)$ such that

$$\frac{\partial F}{\partial u} = \frac{m(u, v, w)}{m(\overline{u}, \overline{v}, \overline{w})}.$$

After the transformation, we have the transformed system

$$\overline{x} = y, \qquad \overline{y} = z, \qquad \overline{z} = G(x, y, z),$$

where

$$G(x, y, z) = \lim_{\varepsilon \to 0} \varepsilon \ln F \left(\exp\left(\frac{x}{\varepsilon}\right), \exp\left(\frac{y}{\varepsilon}\right), \exp\left(\frac{z}{\varepsilon}\right)\right),$$

provided the limit exists. Then

$$\frac{\partial}{\partial x} G(x, y, z) = \lim_{\varepsilon \to 0} \varepsilon \frac{\partial}{\partial x} \left(\ln F \left(\exp\left(\frac{x}{\varepsilon}\right), \exp\left(\frac{y}{\varepsilon}\right), \exp\left(\frac{z}{\varepsilon}\right)\right)\right)$$
$$= \lim_{\varepsilon \to 0} \frac{1}{F\left(\exp\left(\frac{x}{\varepsilon}\right), \exp\left(\frac{y}{\varepsilon}\right), \exp\left(\frac{z}{\varepsilon}\right)\right)} \frac{\partial F}{\partial u} \exp\left(\frac{x}{\varepsilon}\right)$$
$$= \lim_{\varepsilon \to 0} \frac{m\left(\exp\left(\frac{x}{\varepsilon}\right), \exp\left(\frac{y}{\varepsilon}\right), \exp\left(\frac{z}{\varepsilon}\right)\right)}{m\left(\exp\left(\frac{\overline{x}}{\varepsilon}\right), \exp\left(\frac{\overline{y}}{\varepsilon}\right), \exp\left(\frac{\overline{z}}{\varepsilon}\right)\right)} \frac{\exp\left(\frac{x+y+z}{\varepsilon}\right)}{\exp\left(\frac{\overline{x}+\overline{y}+\overline{z}}{\varepsilon}\right)}.$$

This means that the measure density function of the transformed system is

$$M(x, y, z) = \lim_{\varepsilon \to 0} m \left(\exp\left(\frac{x}{\varepsilon}\right), \exp\left(\frac{y}{\varepsilon}\right), \exp\left(\frac{z}{\varepsilon}\right)\right) \exp\left(\frac{x + y + z}{\varepsilon}\right),$$

provided the limit exists. Note that if we have a uniform measure $m(u, v, w) = 1$, the last limit does not exists.

References

[1] Ochiai T 2004 Inversible Max-Plus algebras and integrable systems *Preprint* nlin.SI/0405067 v1

[2] Grammaticos B, Ohta Y, Ramani A, Takahashi D and Tamizhmani K M 1997 Cellular automata and ultra-discrete Painleve equations *Phys. Lett.* A **226** 53–8

[3] Quispel G R W, Capel H W, Papageorgiou V G and Nijhoff F W 1991 Integrable mappings derived from soliton equations *Physica* A **173** 243–66

[4] Quispel G R W, Capel H W and Scully J 2001 Piecewise-linear soliton equations and piecewise-linear integrable maps *J. Phys. A: Math. Gen.* **34** 2491–2503

[5] Quispel G R W, Capel H W and Roberts J A G Duality for discrete integrable systems in preparation

[6] Roberts J A G, Iatrou A and Quispel G R W 2002 Interchanging parameters and integrals in dynamical systems: the mapping case *J. Phys. A: Math. Gen.* **35** 2309–25

[7] Scully J 1999 An exploration of integrable two-dimensional maps *Honours Thesis* Mathematics Department, La Trobe University

[8] Tokihiro T, Takahashi D, Matsukidaira J and Satsuma J 1996 From soliton equations to integrable cellular automata through a limiting procedure *Phys. Rev. Lett.* **76** 3247–50